JOURNAL OF GEOPHYSICAL RESEARCH, VOL. 104, NO. B10, PAGES 23,199–23,213, OCTOBER 10, 1999

Development of an Antarctic digital elevation model by integrating cartographic and remotely sensed data: A geographic information system based approach

Hongxing Liu

Department of Geography and The Byrd Polar Research Center, Ohio State University, Columbus

Kenneth C. Jezek

The Byrd Polar Research Center and Department of Geological Sciences, Ohio State University, Columbus

Biyan Li

The Byrd Polar Research Center, Ohio State University, Columbus

Abstract. We present a high-resolution digital elevation model (DEM) of the Antarctic. It was created in a geographic information system (GIS) environment by integrating the best available topographic data from a variety of sources. Extensive GIS-based error detection and correction operations ensured that our DEM is free of gross errors. The carefully designed interpolation algorithms for different types of source data and incorporation of surface morphologic information preserved and enhanced the fine surface structures present in the source data. The effective control of adverse edge effects and the use of the Hermite blending weight function in data merging minimized the discontinuities between different types of data, leading to a seamless and topographically consistent DEM throughout the Antarctic. This new DEM provides exceptional topographical details and represents a substantial improvement in horizontal resolution and vertical accuracy over the earlier, continental-scale renditions, particularly in mountainous and coastal regions. It has a horizontal resolution of 200 m over the rugged mountains, 400 m in the coastal regions, and approximately 5 km in the interior. The vertical accuracy of the DEM is estimated at about 100-130 m over the rugged mountainous area, better than 2 m for the ice shelves, better than 15 m for the interior ice sheet, and about 35 m for the steeper ice sheet perimeter. The Antarctic DEM can be obtained from the authors.

1. Introduction

Digital elevation models are of fundamental importance to many geoscientific and environmental studies of the Antarctic. Elevation data can be used to infer the locations of ice divides, drainage basins, ice flow direction [*Drewy,* 1983], and grounding lines [*Partington et al.,* 1987; *Ridley et al.,* 1989], and together with ice thickness data, to calculate driving stresses and ice deformational velocity, and to give a measure of subsurface and basal conditions [*Bamber and Bindschadler,* 1997]. Surface topographic measurements can be used as an important input to estimate the surface temperature, precipitation, and katabatic wind intensity and direction [*Marsiat and Bamber,* 1997]. An accurate knowledge of surface topography is also essential for enhancing our ability to use remotely sensed data in mapping and studying the Antarctic [*Jezek,* 1998].

In the past two decades, great efforts have been directed to the development of a continental scale digital elevation model of the Antarctic. *Budd et al.* [1984] constructed a digital elevation model (DEM) with a grid spacing of 20 km based on a digitized 1:6,000,000 scale Scott Polar Research Institute (SPRI) folio map [*Drewy,* 1983]. With the successful launches of U.S. Seasat, Geosat, and European Space Agency's (ESA) ERS-1 satellite, a large volume of accurate radar altimetry measurements over marginal ice shelves and much of the interior of the Antarctic ice sheet have become available [*Zwally et al.,* 1983, 1987; *Ridley et al.,* 1993]. On the basis of Seasat and Geosat radar altimeter data, two DEM grids were derived with a horizontal spacing of 20 and 10 km, respectively [*Zwally et al.,* 1983, 1987]. Their ground coverages are limited to 72°S. Recently, 5 km resolution DEMs have been derived independently by *Zwally et al.* [1997] and *Bamber and Bindschadler* [1997] based on the ERS-1 radar altimeter data. The coverage of ERS-1 radar altimeter data extends to 81.4°S. As a part of the global 30 arc second digital elevation model project (GTOPO30), U.S. Geological Survey (USGS) EROS Data Center created an Antarctic DEM with 1 km grid spacing using the digitized topographic maps [*EROS Data Center,* 1996; *Verdin and Greenlee,* 1996].

The previously published Antarctic DEMs were primarily derived from a single data source. They are characterized by relatively low horizontal resolution and unreliable measurements over the mountainous and highly sloped areas,

Paper number 1999JB900224.
0148-0227/99/1999JB900224$09.00

and/or incomplete coverage. These drawbacks limit their suitability for high-resolution modeling of the Antarctic topography. For example, the Radarsat Antarctic Mapping Project (RAMP) requires a high-resolution DEM to correct terrain distortions of Radarsat synthetic aperture radar (SAR) imagery for producing an orthorectified image mosaic over the entire continent of Antarctica [*Jezek,* 1998]. The previously published DEMs were inadequate for this application.

In this paper, we present a new, complete, seamless DEM of the Antarctic that has spatial resolution ranging from 200 m to 5 km. Our DEM is constructed from a wide selection of topographic data sets, which we have carefully assessed so as to fully exploit the largest-scale, highest-quality data contained in each source. We rely on the most detailed cartographic data in the Antarctic Digital Database (ADD) and large-scale topographic maps from the USGS and Australian Antarctic Division for mountainous and steeply sloping areas. We use a suite of spaceborne radar altimeter data sets over much of the interior ice sheet where surface slopes are low and the absolute accuracy of the radar altimeter is high [*Zwally et al.,* 1983; *Bamber,* 1994]. A considerable volume of airborne radar data is also utilized in the DEM generation process to fill data gaps and enhance accuracy. Our DEM captures the best available digital topographic information. As a result, it provides exceptional details of the varied topography of the continent and is well suited for many geoscientific, environmental, and mapping applications that require high-resolution elevation data, such as the RAMP.

Our DEM generation activities were automated with the aid of a geographic information system (GIS) based toolkit that was developed by using ARC/INFO analytical and graphical functions and C programming language. The toolkit is capable of adjusting planimetric and vertical reference systems of source data, checking and editing source data for error correction, interpolating various types of source data into grid DEM data sets, integrating and merging different data sets, and visualizing the DEM products in various ways [*Liu,* 1999].

2. Data Compilation and Selection

A comprehensive collection of digital topographic source data was compiled with the help of many investigators. These data can be grouped into three categories: cartographic data, remotely sensed data, and survey data.

Cartographic data include contours, spot height points, and surface structure lines digitized from paper topographic map sheets (Table 1). The British Antarctic Survey (BAS) in collaboration with the SPRI and World Conservation Monitoring Center (WCMC) constructed the Antarctic digital database (ADD) [*Cooper,* 1993; *BAS, et al.,* 1993]. The ADD represents the best digital collection of the vector cartographic data over the Antarctic. Of the 210 map sheets digitized, 164 are at the scale of 1:250,000. We used the most detailed data, namely, the original scale of the source topographic maps to which no generalization was applied. To augment the ADD, we acquired large-scale digital topographic maps from the USGS (C. Hallam and J. Mullins, personal communication, 1998) and the Australian Antarctic Division (L. Belbin and U. Ryan, personal communication, 1998), and also digitized one topographic map from Institut für Angewandte Geodäsie of Germany [*Sievers et al.,* 1994] (Table 1).

Remotely sensed data consists of satellite radar altimetry data and airborne radar echo sounding data (Table 2). We received several ERS-1 radar altimeter data sets preprocessed by different investigators. *Ihde et al.* [1995] used 17 sets of 35-day repeat cycle data to generate a DEM with latitude spacing of 0.05° and longitude spacing of 0.2°. *Bamber and Bindschadler* [1997] applied the offset center of gravity method for waveform retracking and the relocation method for slope-induced error correction to two 168-day cycles of the ERS-1 geodetic mission and created a 5 km resolution DEM. *Zwally et al.* [1997] used a 9- or 5-parameter fitting function for waveform retracking and the direct slope correction method for slope induced error correction. On the basis of two 168-day cycles from the geodetic phase and two 35-day cycles from the multidisciplinary mission, a 5-km resolution grid was generated by using a biquadratic function

Table 1. Digital Cartographic Data Sources for Antarctica

Source	Coverage	Scale	Contour Interval, m
ADD	the entire Antarctic continent	Varied	Varied
	Transantarctic Mountains	1:250,000	200
	Ellsworth Mountains	1:250,000	200
	the coastal mountains of Marie Byrd Land and Queen Maud Land	1:250,000	200
	Antarctic Peninsula	1:250,000	250
	Most coastal regions in East Antarctica	1:1,000,000	100
	The interior of the ice sheet	1:3,000,000	200
USGS contour data	Dry Valley region in the Transantarctic Mountains	1:50,000	50
Australian contour data	Vestfold Hills	1:25,000	10
	Larsmann Hills	1:25,000	10
	Windmill Islands	1:50,000	10
German topographic map	Berkner Island, Henry Ice Rise, and Korff Ice Rise	1:2,000,000	100

Table 2. Remotely Sensed Topographic Data for Antarctica

Source	Coverage	Accuracy, m	Density
ERS-1 radar altimeter ice mode data	marginal ice shelves and the ice sheet up to 81.4° S	2-35	about 5 km intervals
ERS-1 radar altimeter ocean mode data	the offshore ocean area	0.1	335 m along track and about 4 km across track
SCP airborne radar sounding data	the upstream parts of ice streams A, B, and C	4-9	120 m along track and 5-10 km across track
BAS airborne radio echo sounding data	Evans ice stream and Fowler Peninsula	6	50-90 m along track and 5-10 km across track
RIGGS airborne and station radar sounding ice thickness data	Ross Ice Shelf	10	contours with a 50 m interval

fitting algorithm. Also, we acquired the ERS-1 altimeter ocean mode data from ESA to derive the mean sea surface height over the offshore ocean area. We obtained two sets of digital airborne radar data. One was originally collected during the 1988-1989 field season of the Siple Coast Project (SCP) [*Retzlaff et al.*, 1993], and the other was collected by BAS (P. Jones, personal communication, 1998). In addition, we digitized an ice thickness map over the Ross Ice Shelf. The map was produced based on airborne and station radar sounding data that were collected during the Ross Ice Shelf Geophysical and Glaciological Survey (RIGGS) [*Bentley and Jezek*, 1981]. We converted the ice thickness data to surface elevation by a linear hydrostatic equilibrium model [*Jenkins and Doake*, 1991].

The survey data include the ground-based survey data and satellite-based Global Positioning System (GPS) measurements. The available ground survey data are mainly from the spot height point layers in the ADD. The spot elevation points contain various types of height measurements, including differential leveling, trigonometrical, airborne altimetric, surface barometric, geodetic satellite observation station, astronomical station, and survey control station [*BAS, et al.*, 1993]. GPS measurements that we assembled consist of several traverses over Siple Dome (T. Scambos, personal communication, 1997), the Lambert Glacier Basin, the Amery Ice Shelf [*Kiernan*, 1998], the Rutford Ice Stream (D. Vaughan, personal communication, 1998), and scattered points in West Antarctica and the Transantarctic Mountains (I. Whillans, T. Wilson, and P. Berkman, personal communication, 1998).

The source data that we compiled have varying coverage, scale, and accuracy. When the source data overlap, we need either to fuse or select the source data. If the overlapped data sources have comparable accuracy and are complementary to each other, we integrate all the source data at the input level. If one data source is absolutely superior to others in terms of accuracy and density, we select the better data source and discard others. Figure 1 shows the distribution of the selected source data used in the final DEM.

We developed the following criteria for data selection based on quality assessments of the source data: (1) use GPS data, airborne radar data, and large-scale topographic maps wherever they are available; (2) use satellite radar altimeter data if surface slope is less than 0.8°; (3) use the ADD cartographic data for rugged and highly sloped areas; and (4) use satellite radar altimeter data for areas with surface slopes between 0.8° and 1.0°, if other data sources are of poor quality or do not agree with the surface shape suggested by satellite image data.

The accuracy of satellite radar altimeter data is strongly correlated with the surface slope and ruggedness. Although the Antarctic Peninsula, most parts of the Transantarctic mountains, and sloping coastal margins are covered by satellite radar altimeter data, the measurements are not reliable or are seriously in error due to poor tracking and the unpredictably complex shape of the waveform. In addition, the slope correction algorithms tend to produce gross errors because of the incorrect estimates of local surface slope. The cartographic data of the ADD in the mountainous and coastal regions are typically at the scale of 1:250,000, originally derived from airborne photogrammetry methods. In comparison, the ADD cartographic data are more reliable and accurate and hence are used as the input source data for computing the DEM in these rugged and highly sloped areas. The Dry Valley region in the Transantarctic Mountains, the Vestfold Hills, the Windmill Islands, and the Larsmann Hills in East Antarctica are covered by large-scale topographic maps collected from the USGS and the Australian Antarctic Division. The scale and spatial resolution are much better than their counterparts in the ADD and are thus used as the sole data source for these areas.

Among several sets of satellite radar altimeter data, we selected the ERS-1 radar altimeter data preprocessed by *Zwally et al.* [1997] because they used more input source data, both two 168-day cycles and two 35-day cycles data, and their result compared favorably with selected independent data. We reserved other ERS-1 data for comparison and verification to increase the reliability of the data. Conventionally, it is recommended that satellite altimetry can be reliably used in the area where the surface slope is less than half the altimeter beam width, 0.65° in the case of ERS-1 altimeter data [*Bamber*, 1994; *Ekholm*, 1996]. However, empirical studies show that after a series of error corrections the radar altimeter can provide reliable measurements over terrain surfaces of up to 0.8°-1.0° slope [*Martin et al.*, 1983; *Zwally et al*, 1983]. *Ekholm* [1996] shows that ERS-1 radar altimeter data are more reliable than the digitized topographic maps on surfaces of up to 1.2° slope in Greenland. We took 0.8° as the basic surface slope threshold for the use of satellite radar altimeter data. In some parts of coastal regions, the use of satellite radar altimeter data was expanded to include surfaces with slopes between 0.8° and 1° on the conditions

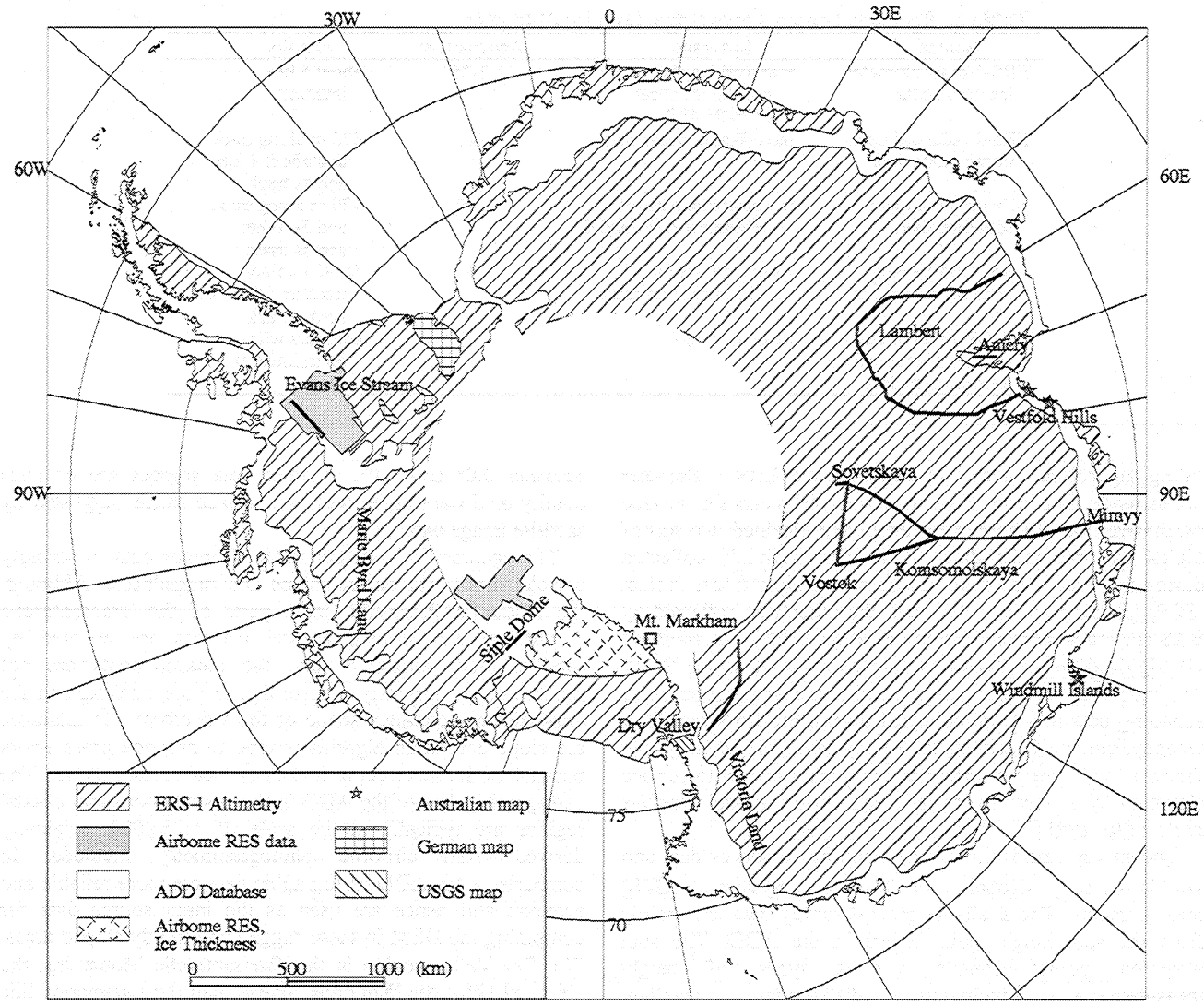

Figure 1. Distribution of input data sources used in final DEM. Dark black lines show the locations of GPS, RES, and geodetic leveling traverses for accuracy assessment in Figure 7 and Table 1. Black box shows the location of the test site Mt. Markham for optimal interpolation spacing determination.

that the cartographic data in the ADD are sparse or simply at odds with the shape indicated by the Advanced Very High Resolution Radiometer (AVHRR) [*Ferrigno et al.*, 1996] and Radarsat Quicklook image mosaics [*Jezek*, 1998]. This expansion mainly occurred in East Antarctica and is supported by the comparison between leveling and GPS traverse data, the ADD contour data, and satellite radar altimetry data.

The interior area south of 81.4°S is not covered by satellite radar altimeter data. We used airborne radar sounding data over the upstream parts of ice streams A, B, and C in West Antarctica because its quality is far superior to the contours in the ADD. Airborne and station radar sounding data acquired by the RIGGS project fills the data gap over the portion of Ross Ice Shelf inside the 81.4°S latitude circle where neither satellite radar altimeter data nor other data sources exist. The cartographic data in the ADD was used for the rest of the area within the 81.4°S latitude circle.

The GPS navigated airborne radar echo sounding data over the Evans Ice Stream and Fowler Peninsula are more accurate and denser than satellite radar altimeter data as well as the ADD contours and therefore are used as the input data for this region. ERS-1 ocean-mode radar altimeter data is used in the offshore ocean area for producing the DEM relative to the World Geodetic System 84 (WGS84) ellipsoid.

3. Data Preprocessing

3.1. Reference System and Data Adjustment

The original source data are provided in different map projections. They are also relative to different vertical datums and have diverse data formats. In order to integrate all the source data, we need to select a common planimetric coordinate system and vertical reference system. To adhere to the recommendations of the Scientific Committee on Antarctic Research (SCAR), the Polar Stereographic projection with a standard latitude of 71°S and a central meridian of 0° is selected as the common planimetric reference system. The coordinates are in meters with the origin at the South Pole.

Most of the cartographic data are referenced to mean sea level (MSL), while the original GPS data, satellite radar altimeter data, and airborne radar data are referenced to the WGS84. Geodetic Reference System 80 (GRS80), WGS72, and Rapp Set A Geoid [*Retzlaff et al.*, 1993] are also used in some source data as the vertical datum. MSL is approximately 1.5 m below the geoid in the Antarctic due to circumpolar currents of the Southern Ocean [*Rapp*, 1991; *Bamber and Bentley*, 1994; *Bamber and Bindschadler*, 1997]. In vertical datum adjustment, we ignored the differences between the MSL elevation and the geoid orthometric height and used the most recent geoid model OSU91A [*Rapp et al.*, 1991] as the common vertical datum to integrate all the source data.

The geoid undulation is calculated from the OSU91A geoid model over the continent and approximated by the mean sea height derived from ocean mode ERS-1 radar altimeter data over the offshore ocean areas. In the Antarctic, the geoidal undulation ranges from –67 to +42 m. We first computed the orthometric DEM grid referenced to the OSU91A geoid from the adjusted source data, then constructed the ellipsoidal height DEM grid relative to the WGS84 ellipsoid by adding the geoidal undulation.

3.2. Error Detection and Correction

We developed a number of GIS-based interactive and semiautomatic techniques for detecting anomalous values and gross errors in source data. As the first step, all the source data were converted into topologically structured ARC/INFO coverages. Our error detection techniques are based on the global and local statistical analyses of the feature attribute tables, topological consistency checking of the local neighborhood, and rapid visualizations of topographic surfaces.

Two major types of errors exist in contour coverages: mislabeled contours and intersections of contours. We identified anomalous elevation labels by statistical analysis of contour coverages. The segments with spurious and irregular elevation labels were displayed and corrected to values inferred from neighboring contours. Next we use a color sequence to visualize a number of adjacent contour lines. A line segment that has a different color from the rest of the contour line or intersects with contour lines of other colors indicates a wrong label or intersection error. Finally, we interpolated the contour coverage into a grid by using the TOPOGRID algorithm [*Hutchinson*, 1989; *Environmental Systems Research Institute (ESRI)*, 1991] and produced a shaded relief image [*Horn*, 1982]. Wrong labels and intersection errors appear as erratic scars, ditches, or sharp peaks and ridges in the shaded relief images. The rejection of artifacts detected in the simulated relief images is justified by comparing with the AVHRR satellite image mosaic [*Ferrigno et al.*, 1996] and Radarsat Quicklook image mosaic of the Antarctic [*Jezek*, 1998]. All the contour coverages from the ADD, the USGS, and the Australian Antarctic Division have undergone these three rigorous checking procedures.

Spot height point coverages were checked and filtered by two steps. First we filtered out negative and extremely large elevation values by using global logical operations on the Point Attribute Tables (PATs) of the coverages. Second we used a cross-validation procedure to check for subtle errors in spot elevation points. Such errors may not show up as global outliers, but their values are strongly inconsistent with those of their neighboring points. We interpolated the elevation values at the positions of spot points from contour coverage and then computed the difference between the interpolated value and spot elevation values. We removed those points that have an absolute difference greater than one contour interval in the relatively flat area and 2 times greater than one contour interval in the rugged area.

Although retracking, slope correction, and other filtering procedures have been applied to the satellite radar altimeter data that we received [*Bamber and Bindschadler*, 1997; *Zwally et al.*, 1997], some errors remain in the data sets. The remaining errors may be caused by poor tracking or complete loss of the returned echo in the original measurements and may be induced by the artifacts of the slope correction and spatial interpolation algorithms. We dropped the erroneous negative values and bad data points flagged by the data contributors by using GIS logical operations. A local consistency check was performed to detect subtle errors that remain undetected as outliers by conventional global statistical methods. For each data point, we calculated the surface slope and the height difference between the original elevation values and the values interpolated from eight adjacent neighbor points. If the slope or the height difference exceeds 3 times the standard deviation from their respective local trend, the corresponding point is flagged as a local outlier and discarded [*Liu*, 1999]. Next the satellite radar altimeter data are interpolated and rendered by the analytical hill-shading method [*Horn*, 1982] with a high vertical exaggeration. Random errors can be detected as spurious and erratic pits or peaks in the shaded relief images. Similar error checking procedures were also applied to airborne radar echo sounding data.

4. DEM Generation Approaches

4.1. Spatial Interpolation Algorithms

The performance of different interpolation algorithms is strongly dependent on the pattern, density, and format of source data [*Liu*, 1999]. The evaluation and choice of interpolation techniques are based on three considerations. First the interpolated surface should agree with the source data well in terms of values and pattern. For contour data we converted the interpolated grid DEMs back to contour lines using half of the original contour interval and then overlaid the derived contour lines on the top of original contour lines to check the consistency. Second the interpolated surface should be single-valued, continuous, and smooth at all positions. Practically, we check the visual plausibility of the resulting terrain surface using analytical hill-shading or the simulated stereo images [*Liu*, 1999], which must be artifact-free and in good agreement with the shape suggested by satellite images. Third the computation involved in interpolation must be efficient and fast in view of the size of the Antarctic continent and the correspondingly large amount of data involved.

4.1.1. Interpolation of satellite radar altimeter data. The satellite radar altimeter data that we received have already been preprocessed into evenly distributed points with about 5-km spacing. Most interpolation algorithms work well for further interpolation of the preprocessed satellite altimeter data. We selected the Triangulated Irregular Network (TIN)

quintic interpolation method due to its computational efficiency. It starts with the Delaunay triangulation of satellite altimeter data points to form triangle patches. A bivariate fifth-degree polynomial is fitted for small surface patches, and then elevation values at nodes of a grid are estimated by evaluating the fitted functions:

$$Z(x,y) = \sum_{j=0}^{5} \sum_{k=0}^{5-j} q_{jk} x^j y^k \quad (1)$$

where $Z(x,y)$ is the interpolated value at the location (x, y) and q_{jk} are the fitted coefficients. The resulting surface looks smooth and realistic because the second derivatives of the surface from TIN quintic interpolation are continuous and differentiable.

4.1.2. Interpolation of traverse airborne radar data. The airborne radar data are anisotropically distributed, namely, densely sampled, along flight lines but widely separated between flight transects. For example, the airborne radar data over ice streams A, B, and C have a sampling interval of about 120 m along track, but the distance between tracks is as large as 5-10 km. This pattern imposes serious difficulties on most general purpose interpolation algorithms [*Liu,* 1999]. We developed a procedure that combines quadrant neighborhood-based Inverse Distance Weighting (IDW) and TIN methods and achieved a reasonable result. First we reduced and filtered airborne radar data along flight lines. A super-block based two dimensional (2-D) searching algorithm was used to partition the data points into an array of square blocks with a width of one-fifth of the average distance between flight lines. For each block, only the median point was selected for subsequent interpolation. On the basis of the retained data points, a coarse grid with a spacing of half the average distance between flight lines was then interpolated by the IDW algorithm. The IDW algorithm uses 12 nearest neighboring points equally selected from each of four quadrants to determine the elevation value:

$$Z_{i,j} = \frac{\sum_{p=1}^{p=12} Z_p d_p^{-n}}{\sum_{p=1}^{p=12} d_p^{-n}} \quad (2)$$

where Z_{ij} is the computed elevation at the node (i, j) of a grid, Z_p is the elevation at point p in the neighborhood, d is the distance from the node (i, j) to point p, and n is the power factor of distance. The inverse squared distance weighting is used (n=2). Finally, we constructed a TIN quintic model using the reduced radar altimeter data together with the IDW derived coarse grid points and interpolated them into a fine DEM grid. The quadrant neighborhood-based IDW interpolation serves to avoid the directional bias and stabilize the interpolation result, while the triangulation of the reduced along track radar data and intermediate coarse grid can retain the topographic details present in the source data.

4.1.3. Interpolation of contour-based cartographic data. Contour data are characterized by the oversampling of information along contour lines and the undersampling between contour lines, especially in low-relief areas with widely spaced contours. It is the most difficult data type for general-purpose interpolation techniques. We tested three contour-specific interpolation algorithms that have appeared in the literature: a TIN-based method [*Auerbach and Schaeben,* 1990; *Robinson,* 1994], the linear gradient descent interpolation method [*Yoeli,* 1984; *Oswald and Raetzsch,* 1984], and the TOPOGRID-based method [*Hutchinson,* 1989; *ESRI,* 1991; *Gesch and Larson,* 1996]. Among them, the TOPOGRID-based method is the most effective in terms of the consistency with the source contour data and the preservation of the fine surface structures [*Liu,* 1999].

The TOPOGRID method is based on *Hutchinson*'s [1989] sophisticated implementation of an iterative finite-difference algorithm. The sample points are allocated to the nearest grid cell, and values at grid cells not occupied by data points are calculated by Gauss-Seidel iteration with overrelaxation subject to a rotation invariant roughness penalty [*Hutchinson,* 1989]. The minimization of the roughness function leads to the minimum curvature interpolation of a thin plate spline. The tendency of the minimum curvature of a thin plate spline to smooth out the ridges and valleys is corrected in TOPOGRID by means of enforcing linear interpolation along all ridge lines and stream lines, which are automatically derived from points of locally maximum curvature on contour lines.

One drawback of TOPOGRID is fictitious overshoots or undershoots in the areas where the contour density has a sharp change. For example, spurious undershoots are generated in areas where the contours are sparse, and there is a steep relief nearby, notably in the low-slope floors of U-shaped glacial valleys flanked by steep glacier shoulders. This problem has also been observed and reported by others [*Bliss and Olsen,* 1996]. The tendency of minimum curvature interpolation to maintain regional trends away from data points is the cause of the problem. To deal with this problem, we designed a modified two-stage TOPOGRID interpolation method. At the first stage, we densify the contour lines in low-slope regions. A very coarse grid is first interpolated from contour lines using the TOPOGRID algorithm. Then the surface slope is calculated, and continuous low slope regions are delineated using a region-growing algorithm [*Liu,* 1999]. The density of contour lines is increased by 4 times in the low-slope regions by converting the coarse grid of the selected low-slope regions into contour lines using one-fourth of the original contour interval. At the second stage we integrate all available input data to create a final high-resolution DEM grid. The input data include the original contours, the densified contours in the low-slope regions, spot elevation points, grounding lines, and coastlines. Streamlines and lake shorelines in coastal mountains identified in the ADD are also used to constrain the interpolation where they are available. The elevation of coastlines is set to zero. The grounding lines, indicating the locations where terrain surface changes from relatively flat ice shelves to the sloped coastal margins of the ice sheet, are used as important structural lines in interpolation. They are first divided into small segments, and then the segments are matched with the nearest satellite radar altimeter data points in ice shelves. The elevation value of the nearest point is transferred to the corresponding grounding line segment.

This modified two-stage TOPOGRID method leads to a topographically correct DEM with several desirable properties. First, fine structures of the topographic surface contained in the original source data are preserved and enhanced in the resultant DEM. This is because the replacement of the minimum curvature constraint with linear

gradient descent interpolation in the TOPOGRID algorithm allows the fitted surface to have sharp changes in slope along surface structural lines and because a significant amount of surface morphologic information was incorporated in the interpolation, including ridge and valley lines automatically derived from contours, grounding lines, and surface peaks in spot height data sets. Second, owing to the surface smoothness constraint imposed by the minimum curvature of a thin plate spline, the resulting surfaces are continuous and differentiable and hence visually smooth and realistic. Third the densification of contour lines in low-relief regions alleviates or eliminates the artificial pits. The reliability and effectiveness of this procedure is shown by comparison of the interpolated contours with original contours in Figure 2, where the interpolated contours are twice as dense as the original ones. Those with common elevation labels are indistinguishable from the original ones, while those with intermediate elevation labels are consistent with the originals in shape and pattern.

4.2. Determination of DEM Grid Spacing

The horizontal grid spacing (cell size) of DEMs is an important parameter that we have to specify during interpolation. Technically, we can interpolate the source data into a grid with an arbitrarily small horizontal spacing. On the one hand, if the grid spacing is too small, the data volume will expand rapidly and artifacts will also be introduced. On the other hand, if the grid spacing is too big, we will lose information contained in the original source data. Therefore we need to pursue an optimal interpolation spacing at which we can minimize the data volume and subsequent computational cost without a significant loss of topographic information. According to the information content of topographic source data and the complexity of terrain surface,

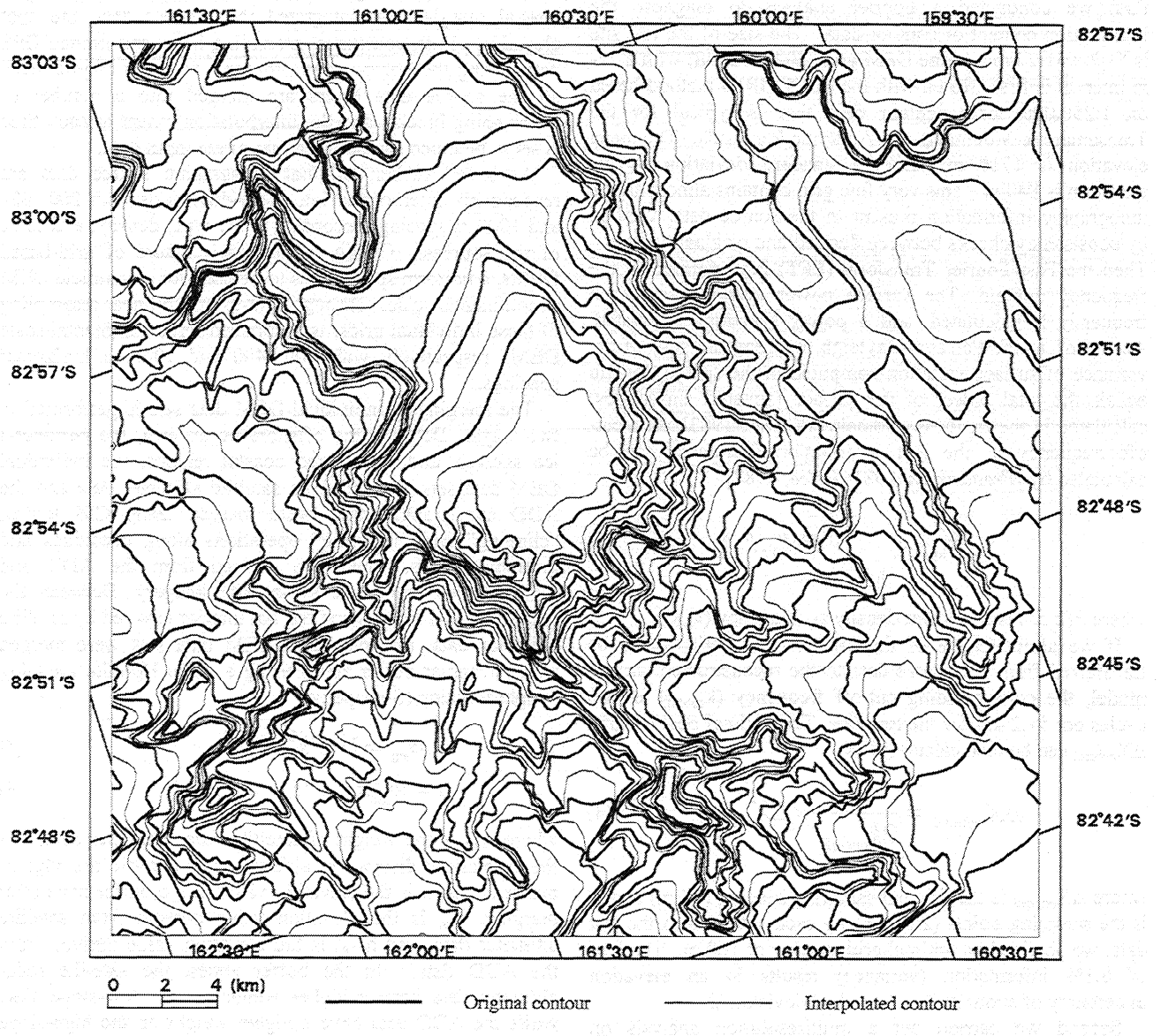

Figure 2. Comparison of interpolated contours from the TOPOGRID algorithm with original contours. Original contours have an interval of 200 m, and the interpolated contours have an interval of 100 m, which are superimposed on the original contours.

we determined an appropriate interpolation spacing for each type of source data. In general, a small grid spacing is required to obtain an accurate representation of the surface details for a rugged and mountainous terrain, while a large grid spacing is sufficient for a low-relief terrain.

The level of topographic detail present in point-type data is dependent upon the density and pattern of the data. We used a grid spacing of 1 km for further interpolation of the preprocessed satellite radar altimeter data and the airborne radar data. This is smaller than half the average distance of preprocessed satellite altimeter data points (2.5 km). It should be noted here that the use of a smaller interpolation spacing cannot increase the original spatial resolution of the source data, but it does prevent loss of detail.

In the case of contour data, the amount of topographic information content is determined by the quality of the original measurements, the map scale, and contour interval. We performed two analyses on a test site around Mt. Markham in the Transantarctic Mountains for the determination of an appropriate grid spacing for interpolation. First we conducted a Fourier analysis to diagnose the information content of contour data. The size of the test site is 51.2 x 51.2 km. A fine DEM grid (2048 x 2048) with a 25-m interval is first created with the TOPOGRID method based on 1:250,000 scale contour data that is typical for the Transantarctic Mountains and Antarctic Peninsula. The mean elevation is 1710 m, and the standard deviation of the elevation is 840 m. This very fine grid contains almost all the topographic information present in the source data, verified by consistency checks between derived and original contours. Then the Fast Fourier Transform (FFT) is performed in the frequency domain. The surface power (variance) at each frequency is calculated, and a power spectrum is created. According to the Parseval-Rayleigh theorem, the sum of the variance of surface variation computed in the spatial domain equals the total power of the surface (squared amplitudes) calculated in the frequency domain [*Weaver*, 1983]. At a cut-off frequency k, the lost information (variance) can be calculated by [*Frederiksen*, 1981; *Balce*, 1987]

$$\sigma^2_{\text{lost}} = \sum_{k_1=k_2=k_{\text{cut-off}}}^{N/2} P(k_1, k_2) \tag{3}$$

where $P(k_1,k_2)$ is the power density at frequency (k_1,k_2).

If we allow 99.9% of the information (variance) to be transferred from the source data to the reconstructed surface model, the corresponding cut-off frequency ($k_{\text{cut-off}}$) is 160 cycles per 51.2 km for the test data. The optimal post spacing $\Delta X_{\text{optimal}}$ can be then calculated as

$$\Delta X_{\text{optimal}} = \frac{N}{2k_{\text{cut-off}}} \times \Delta X_{\text{original}} \tag{4}$$

where $\Delta X_{\text{original}}$ is the original sampling spacing (25 m) and N is the sampling points (2048) along each side. From the test data, we obtained an optimal grid spacing of 160 m. The loss of 0.1% information (variance) results in an elevation uncertainty of about 26.5 m (standard deviation).

Second we carried out a multiresolution analysis on interpolation errors against the different grid spacings. For the same test data, we interpolated the contour data respectively into 50, 100, 200, 400, 800, 1600, and 3200m grids using the TOPOGRID algorithm and then calculated the difference between these coarse DEM grids and the 25 m DEM grid, which is used as the base reference grid. The average height difference is used as a measure to quantify the interpolation errors caused by using a larger grid spacing. The error is found to increase linearly with grid spacing. The 200-m grid spacing corresponds to an average height error of 16.4 m.

On the basis of the above analyses, we decided to use 200 m as the interpolation grid spacing for mountainous areas where 1:250,000 scale contour data are available. It should be noted that the test area is one of the most rugged areas in the Antarctic, where the contour density is very high. For the sloped coastal area, the contours are relatively smooth and regular, so a 400-m grid spacing is used instead, which is again supported by comparing the derived contours with original contours.

4.3. Data Integration

We conducted data integration and merging both at the input and output stages. For the mountainous and sloped coastal margins, we integrated the contour data, the spot elevation points, coastlines, grounding lines, and limited GPS data during the interpolation process. To avoid edge effects, all the source data layers are merged into a number of overlapping blocks, and the interpolation extent at each time is set to be much smaller than that of the input data.

As stated earlier, original topographic source data are respectively interpolated into individual grids with 200, 400 and 1000 m spacings according to the type, density, and scale of the sources. Owing to the raster nature of grid-based DEMs, a uniform spacing has to be used for a complete DEM at continental scale. Through grid-to-grid bilinear resampling of these individual grids, we produced three continental scale DEMs respectively with 200, 400 and 1000 m horizontal spacings.

The merging of individual DEM data sets is performed in two ways. Between the offshore ocean area, the peripheral ice shelves, and the rugged coastal regions, the individual DEM data sets, derived from satellite altimeter data and the ADD cartographic data, were merged using GIS logical "clipping" and "inserting" operations along coastlines and grounding lines, which are derived from the ADD and modified with reference to satellite imagery. Between the rugged coastal regions and the flat interior covered by satellite altimeter data, the individual DEM data sets were merged along irregular buffer zones using a cubic Hermite blending weight function (S-shaped):

$$w_{\text{sat}} = 1 - 3s^2 + 2s^3 \tag{5}$$

$$h = w_{\text{sat}} h_{\text{sat}} + (1 - w_{\text{sat}}) h_{\text{ADD}} \tag{6}$$

where w_{sat} is the weight of satellite radar altimeter data, s is the normalized distance of altimeter data point to the edge of buffer zones, h is the elevation value in the buffer zone after merging, h_{sat} is the elevation value derived from satellite altimeter data, and h_{ADD} is the elevation value derived from the ADD data. In the buffer zones, the satellite radar altimeter data have a higher weight on the low-slope side, while the ADD data have a higher weight on the high-slope side. The transitional buffer zones are about 10 km wide, and their locations are determined by the surface slope of 0.8°-1.0°, the threshold value for the use of satellite radar altimeter data.

5. Analysis of the Resultant DEM

5.1. Information Content and Validation

Figure 3 is a hill-shaded image constructed from our DEM at the continental scale. It shows the overall topography of the Antarctic, including the ice divides, glacial drainage basins, ice shelves, ice rises, coastal margins, mountain chains, and volcanoes. It also captures more subtle features, such as the McMurdo Dry Valleys, Lake Vostok, ice flow lines on the Ross Ice Shelf and Ronne-Filchner Ice Shelf, and textured structures probably related to subglacial topography.

A simple qualitative validation of the DEM was obtained by extracting ice drainage basins and ice flow lines. We first removed the high-frequency topographic components from our 1000-m DEM grid by a low-pass Gaussian filter with a window of 25-km radius. The ice divides are delineated based on the ridgelines between ice basins by using an automatic algorithm in ARC/INFO [*Liu,* 1999]. Ice flows along the direction of steepest decent in surface elevation, namely, the aspect of the terrain surface. On the basis of this principle, an algorithm is developed to derive ice flow lines. We first generate a series of seed points on both sides of the ice divides within a narrow buffer zone and then trace the ice flow line downslope from each seed point in a series of small (3-km) steps. To make the algorithm robust to random errors in aspect calculation, the previous step direction is stored in memory. If the current direction is different from the previous direction by 45°, the previous direction is used. The tracking procedure for each seed point is terminated when the flow line reaches the coastlines or meets other flow lines (Figure 4).

Visual inspection shows that the locations and directions of the flow lines are consistent with the terrain features in satellite images, and most of the flow lines converge into major ice streams or outlet glacier channels as indicated by satellite images. The ice divides and ice flow lines derived from our DEM provide great detail about the ice drainage pattern in comparison to the earlier ice drainage map of *Drewry* [1983].

In addition to the broad topographic configuration and the true ice drainage pattern, our high-resolution DEM contains considerable information about small-scale terrain

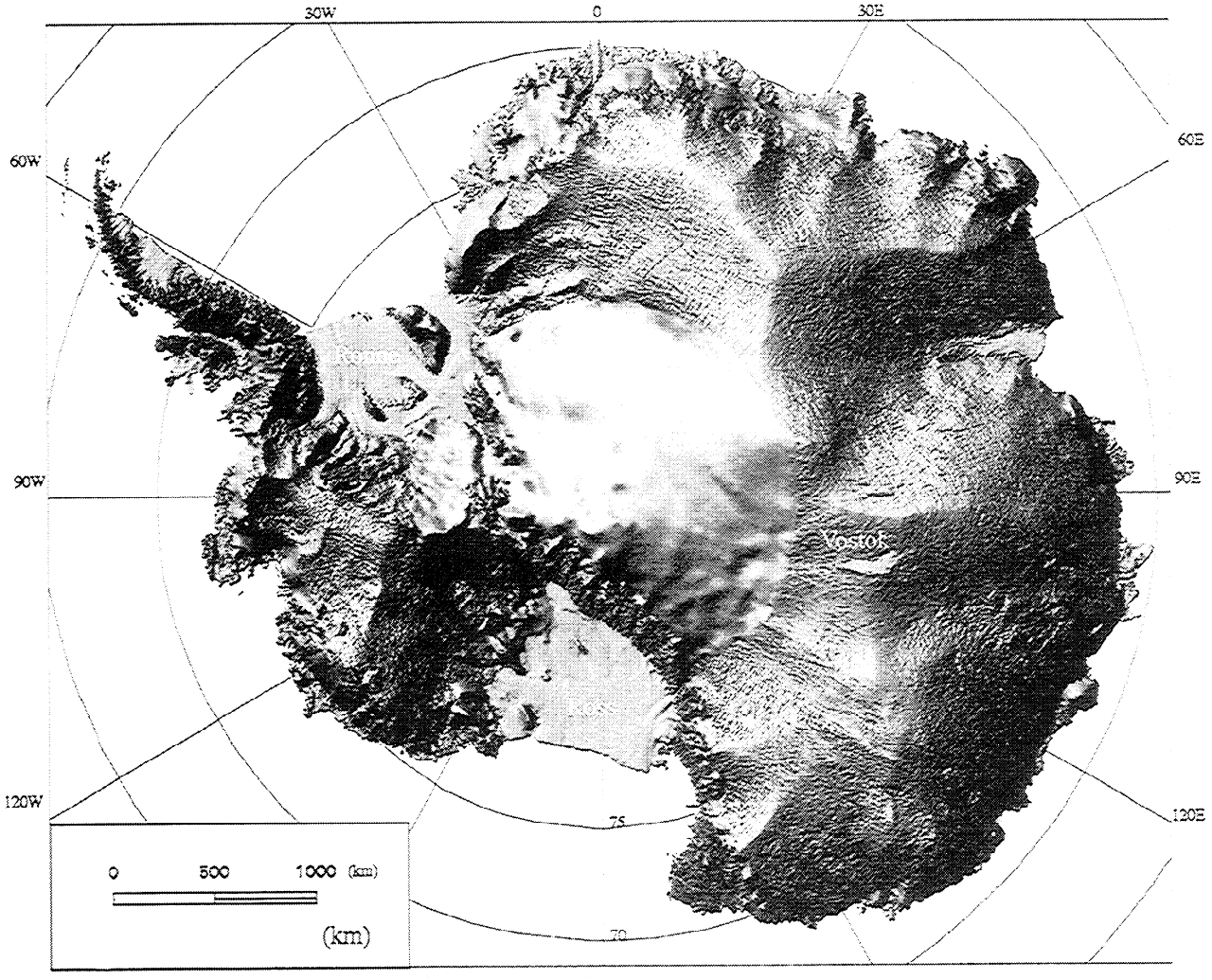

Figure 3. Shaded relief image of the DEM at the continental scale.

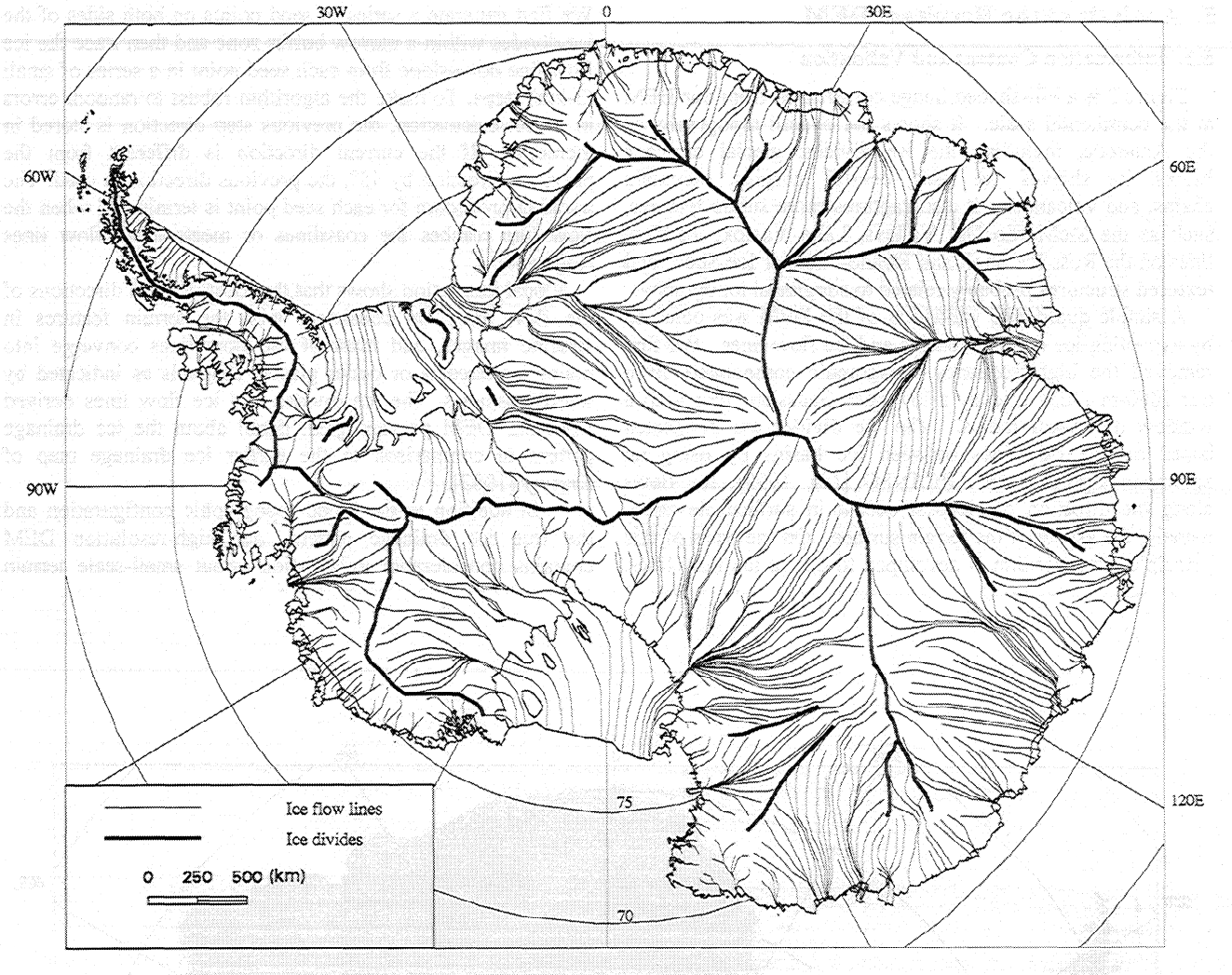

Figure 4. Ice drainage pattern and ice flow lines derived from Antarctic DEM.

features. This is demonstrated by the comparison of our DEM with high-resolution satellite images [*Liu,* 1999], including a LANDSAT thematic mapper (TM) image, a declassified intelligence satellite photography (DISP) [*McDonald,* 1995], and Radarsat SAR images. Figure 5 compares a hill-shaded image derived from the DEM with a DISP satellite photograph near the Beardmore Glacier in the Transantarctic Mountains. The DEM simulated relief image presents a clear picture of morphologic features and surface undulations. The shapes and orientations of major glacial valleys and mountain ranges derived from the DEM (200-m resolution) match very well with those observed in the DISP satellite photograph (about 150-m resolution). Figure 6 shows a terrain-corrected Radarsat SAR image (25-m resolution) draped on the top of the DEM of the Pennell Coast. The elevation data of the DEM is in good agreement with the terrain features in the SAR image, demonstrating the capability of our DEM to rectify and visualize the high-resolution satellite imagery in rugged areas.

5.2. Horizontal Resolution and Positional Accuracy

Though we produced three sets of continental-scale DEMs with grid spacings of 200, 400 and 1000 m, the real horizontal resolution of the DEMs varies from place to place according to the density and scale of the original source data. By diagnosing the information content of original source data, the horizontal resolution of our DEM is estimated at about 200 m in the Transantarctic Mountains and Antarctic Peninsula and about 400 m in the sloped coastal regions. For the ice shelves and the inland ice sheet covered by satellite radar altimeter data, the horizontal resolution remains about 5 km. Where the airborne radar sounding data were used, the horizontal resolution is estimated at about 1 km. The flat plateau inside 81.5°S has a small-scale contour coverage, and the horizontal resolution is estimated to be at about 10 km.

Positional accuracy of the DEM is also evaluated in a number of selected areas by comparison with orthorectified high-resolution satellite images. In general, the absolute planimetric accuracy of topographic features extracted from the DEM is better than 100-300 m. An exception is the Ellsworth Mountains. Comparison of the simulated relief image from the DEM with an orthorectified Landsat image and a Radarsat SAR image in this region revealed that the source contours of the ADD have 3-5 km positional offsets, although the shapes of terrain derived from the DEM closely match the satellite images [*Liu,* 1999]. The positional error was most likely caused by the poor ground control and

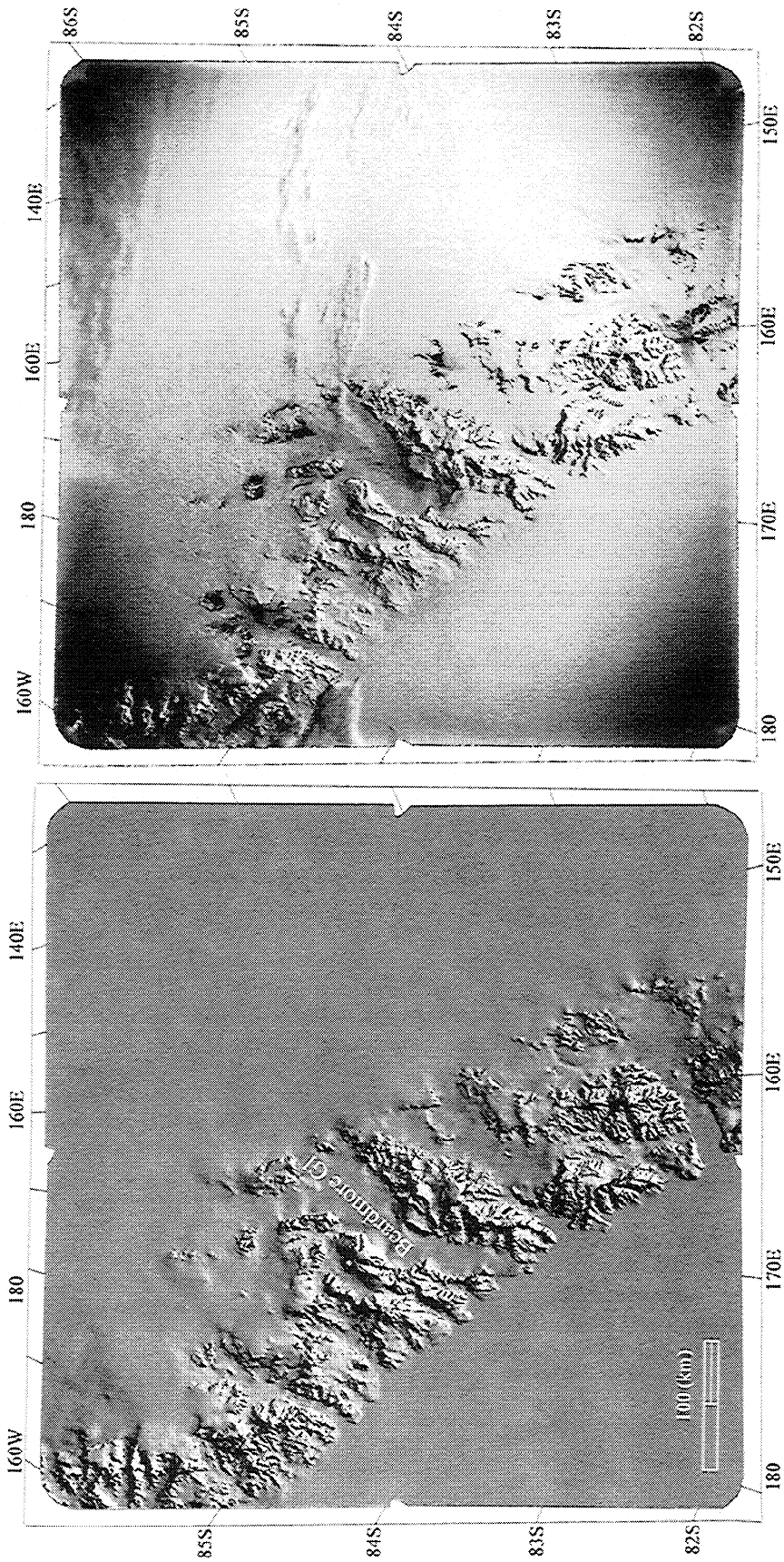

Figure 5. Comparison of the DEM shaded relief image with DISP satellite photograph near Beardmore Glacier. (a) Hill-shaded image from DEM (200 m resolution) and (b) DISP satellite photograph (150 m resolution).

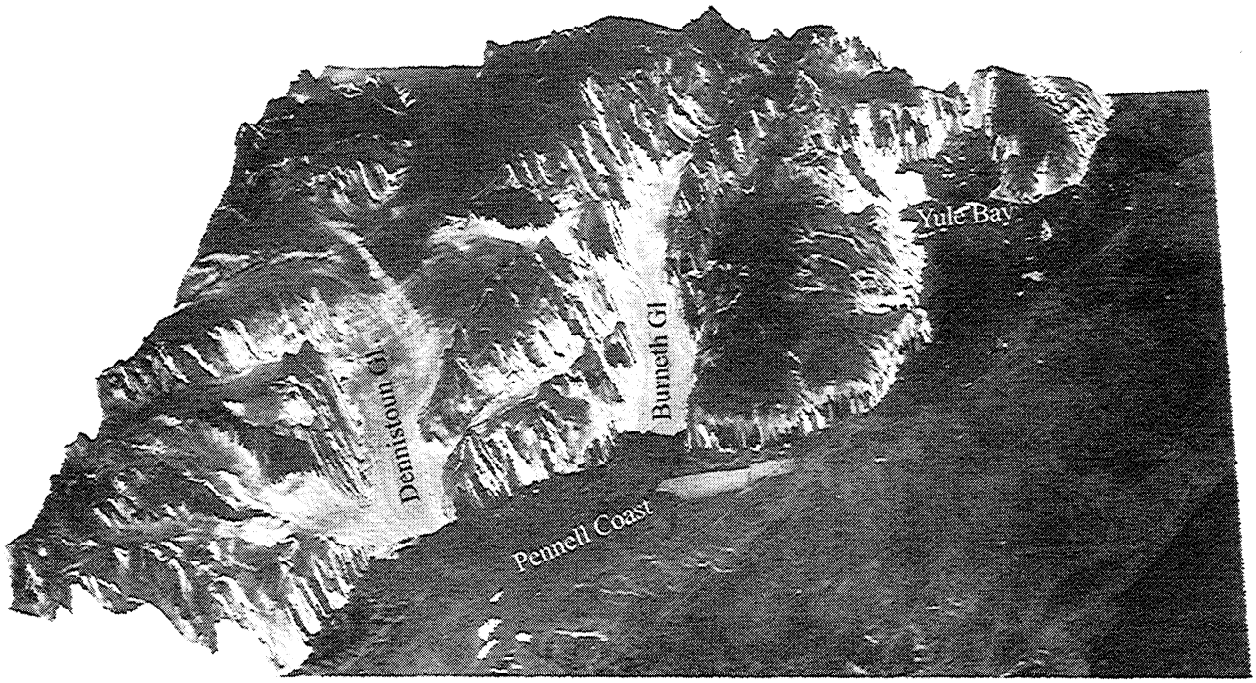

Figure 6. Perspective view of Radarsat SAR image draped on the DEM of Pennell Coast, Victoria Land.

inaccurate navigation technique during the 1960s when the topographic maps were produced. We corrected this positional error by a warping technique based on several selected tie points.

5.3. Vertical Accuracy

Absolute vertical accuracy of our DEM varies with location according to the source data and the terrain complexity. Practically, all available high-quality topographic information was included in our DEM generation. However, we can find a realistic estimate of vertical accuracy by omitting the measurements of high accuracy from the DEM creation and using them as ground truth instead. In our accuracy analysis, the mean, standard deviation and root mean squared error (RMSE) are used to quantify the nature and magnitude of errors. The mean represents a systematic shift between the measured and true surfaces, and the standard deviation is the dispersion of measurement errors. If there is no systematic error, namely, the mean is zero, then the standard deviation equals the RMSE.

The accuracy of the grid DEM derived from the ADD is mainly influenced by the quality of the original measurements, the map scale, and contour interval (Table 1). For the dry valley region, one of the most rugged areas in the Antarctic, we compared the DEM grid derived from the ADD 1:250,000 scale contour data with the USGS 1:50,000 scale contour data that are assumed accurate to represent the ground truth. The mean of the error is 75 m with standard deviation of 109 m, and the RMSE is 132 m [*Liu and Jezek,* 1999].

We also compared the elevation values of the DEM with GPS traverses over Lambert Glacier Basin, Amery Ice Shelf, and Siple Dome, with a GPS-navigated airborne RES traverse over the Evans Ice Stream, with Soviet geodetic leveling traverses, and with a barometric altimetry traverse over Victoria Land (Figure 7 and Table 3). The Lambert Glacier Basin GPS traverse route consists of 73 data points at about 30 km intervals [*Kiernan,* 1998]. The elevation values in the DEM derived from ERS-1 radar altimeter data are in good agreement with the GPS measurements (Figure 7a). The Amery Ice Shelf GPS traverse was selected from a denser kinematic GPS survey data set [*Phillips et al.,* 1996]. Thirteen GPS corner points in the middle of the Amery Ice Shelf with a spacing of 10 km were selected for comparison. As shown in Figure 7b, the ERS-1 radar altimeter derived elevation values in the DEM agree with the kinematic GPS measurements to within 2 m. The Siple Dome GPS traverse is about 120 km long, where the DEM data is derived from the cartographic data in the ADD. The RMSE of the error along the Siple Dome traverse is about 20 m (Figure 7c). The selected Evans Ice Stream airborne RES traverse is about 240 km long. If we ignore the airborne radar echo sounding data and only use the satellite radar altimeter data in this area, the corresponding RMSE is 33 m (Figure 7d). The Soviet geodetic leveling measurements were carried out during the Fourth and the Sixth Soviet Antarctic Expedition. The original measurement error for the Mirnyy-Komsomolskaya (880 km) traverse is about 3-5 m [*Shcheglov,* 1965], and the error in closing the Komsomolskaya-Sovetskaya-Vostok-Komsomolskaya triangular loop (1500 km) is 6.5 m [*Lazarev,* 1966]. As indicated in Figure 7e, our DEM agrees with the Soviet geodetic leveling data very well, and the RMSE value is 13 m (Table 3). The Victoria Land barometric altimetry traverse data were extracted from the ADD spot height coverage. The RMSE between our DEM and the Victoria barometric data is 14 m (Figure 7f).

6. Discussion and Conclusion

This paper presents a high-resolution digital elevation model for mapping and studying the geomorphologic

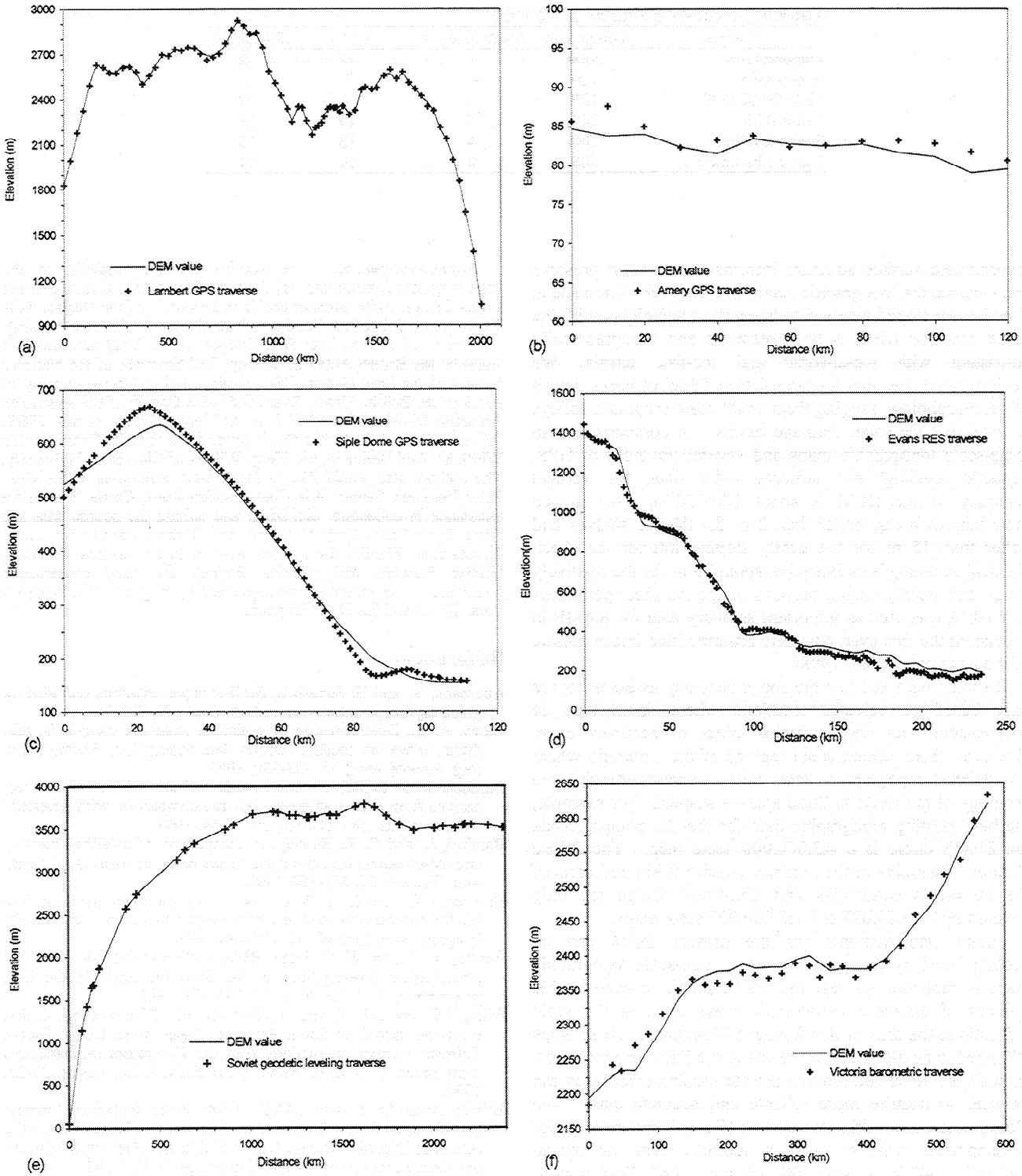

Figure 7. Accuracy assessment of the DEM by comparing with GPS, RES, and leveling data. (a) Lambert Glacier Basin GPS traverse, (b) Amery GPS traverse, (c) Siple Dome GPS traverse, (d) Evans Ice Stream RES traverse, (e) Soviet geodetic leveling traverse, (f) Victorial Land barometric altimetry traverse.

characteristics and dynamic behavior of the Antarctic. It covers the entire Antarctic continent and its surrounding offshore ocean area in a polar stereographic projection with reference to both the OSU91A geoid and the WGS84 ellipsoid. Unlike previous DEMs, our DEM is constructed by integrating the widest variety of topographic source data in a GIS environment. By combining the comparative advantages of available sources, we fully exploited the most detailed and accurate topographic information in each data set. We carried out extensive and rigorous error checking procedures, which make our DEM highly reliable and free of gross errors. We designed sophisticated interpolation algorithms and

Table 3. Accuracy Estimates of the DEM

Traverse	Length, km	Mean Error, m	s. d., m	RMSE, m
Lambert GPS	2000	1	12	12
Amery GPS	120	-1	1	2
Siple Dome GPS	120	-6	18	19
Evans RES	240	15	29	33
Soviet leveling	2380	4	13	13
Victoria barometric	600	0	14	14

incorporated surface structure information so as to preserve and enhance the topographic details present in the source data. We also developed a new data integration technique, with the result that our DEM is both seamless and topographically consistent with ice-covered and ice-free terrain. We demonstrated that this high-resolution DEM captures details of geomorphology ranging from small-scale mountain valleys to extensive ice sheet drainage basins. In comparison with large-scale topographic maps and several traverses of GPS, geodetic leveling, and airborne radar data, the vertical accuracy of the DEM is about 100-130 m over rugged mountainous areas, better than 2 m for the ice shelves and better than 15 m for the gently sloping interior ice sheet. Vertical accuracy is estimated at about 35 m for the relatively rough and steeply sloped portions of the ice sheet perimeter. Our DEM was used as important ancillary data for RAMP in producing the first ever, complete orthorectified image mosaic of the Antarctic [*Jezek*, 1998].

It should be noted that the above accuracy assessments are only based on selected locations where some type of independent data with a higher order of accuracy exist. However, there remain some regions of the Antarctic where no reliable topographic data exist. Correspondingly, the accuracy of the DEM in these areas is suspect. For example, the best existing topographic data for the flat plateau inside the 81.4°S circle is a 1:3,000,000 scale map. The Prince Charles Mountains in the Lambert Glacier Basin and parts of the Pensacola Mountains and Shakleton Range are only covered by 1:1,000,000 and 1:3,000,000 scale maps.

Future improvements for the present DEM can be accomplished by incorporating more large-scale topographic maps in mountainous regions. For example, a considerable number of Japanese topographic maps exist at the scale 1:50,000 in the area of Sør Rondane Mountains. These maps still need to be digitized for the use in the DEM enhancement. In addition, advanced satellite remote sensing techniques can be used to acquire more reliable and accurate data. The Geoscience Laser Altimeter System (GLAS), presently under development, will fly onboard ICESAT with an orbital inclination 94° in the year 2001 [*Schutz*, 1998]. With a small footprint of 70 and 170 m sampling spacing along track, GLAS will provide accurate and dense measurements over the Antarctic up to the latitude of 86°S. Our initial experiments also show that the shape-from-shading, SAR stereo, and InSAR techniques can be used to further improve both the resolution and accuracy of our Antarctic DEM [*Liu*, 1999]. We have established a GIS-based database to maintain all the topographic source data for each portion of the DEM. Consequently, as new data become available, it is practical to continually update the DEM and guarantee that our DEM product is the best and most timely representation of Antarctic topography.

Acknowledgments. The authors are very grateful to the following data contributors: Jay Zwally of the NASA Goddard Space Flight Center; Anita Brenner and John DiMarzio of the Hughes STX Corporation; Johnathan Bamber of the Center for Remote Sensing, University of Bristol, UK; Paul Cooper, David Vaughan, and Phil Jones of the British Antarctic Survey; Ted Scambos of the National Snow and Ice Data Center, USA; Craig Lingle of the University of Alaska; Lee Belbin, Ursula Ryan, and Mike Craven of the Australian Antarctic Division; Cheryl Hallam and Jerry Mullins of the USGS; Johannes Ihde of the Intitut für Angewandte Geodäsie, Germany; Ian Whillans, Paul Berkman, and Terry Wilson of Ohio State University. The authors also would like to thank their colleagues at the Byrd Polar Research Center: Ada Chan, Braden Love, Carrie Dratwa for assistance in collecting, digitizing, and editing the source data and Hong-Gyoo Sohn, Katy Notimier, and Richard Forster for useful discussions. Finally, the authors want to thank Andrew Fountain, Gwenn Flowers, and Charles Bentley for their constructive comments. The research was supported by a grant from NASA's Polar Ocean and Ice Sheet Program.

References

Auerbach, S., and H. Schaeben, Surface representations reproducing given digitized contour lines, *Math. Geol., 22*, 723-742, 1990.

Balce, A. E., Determination of optimum sampling interval in grid digital elevation models (DEM) data acquisition, *Photogramm. Eng. Remote Sens., 53*, 323-330, 1987.

Bamber, J., A digital elevation model of the Antarctic ice sheet derived from ERS-1 altimeter data and comparison with terrestrial measurements, *Ann. Glaciol, 20*, 48-54, 1994.

Bamber, J., and C. R. Bentley, A comparison of satellite-altimetry and ice-thickness measurements of the Ross Ice Shelf, Antarctica, *Ann. Glaciol., 20*, 357-364, 1994.

Bamber, J. L., and R. A. Bindschadler, An improved elevation data set for climate and ice-sheet modeling: Validation with satellite imagery, *Ann. Glaciol., 25*, 430-444,1997.

Bentley, C. R., and K. C. Jezek, RISS, RISP and RIGGS: Post-IGY glaciological investigations of the Ross Ice Shelf in the U.S. programme, *J. R. Soc. N. Z., 11*, 355-372, 1981.

Bliss, N.B., and L.M. Olsen, Development of a 30-arc-second digital elevation model of South America, paper presented at Pecora Thirteen Human Interactions with the Environment-Perspective from Space, U. S. Geol. Surv., Sioux Falls, S. D., August 20-22, 1996.

British Antarctic Survey (BAS), Scott Polar Research Institute (SPRI), and World Conservation Monitoring Center (WCMC), Antarctic Digital Database User's Guide and Reference Manual, Sci. Comm. on Antarctic Res., Cambridge, U. K., 1993.

Budd, W.F., D. Jenssen, and I.N. Smith, A three-dimensional time-dependent model of the Antarctic ice sheet, *Ann. Glaciol.*, 5, 29-36, 1984.

Cooper, A.P.R., J.W. Thomson, and E.M. Edwards, An Antarctic GIS: The first step, *GIS Europe, 2*(6), 26-28, 1993.

Drewry, D., *Antarctica: Glaciological and Geophysical Folio*, Scott Polar Res. Inst., Univ. of Cambridge, Cambridge, U. K., 1983.

Ekoholm, S., A full coverage, high-resolution, topographic model of Greenland computed from a variety of digital elevation data, *J. Geophys. Res., 101*, 21,961-21,972, 1996.

Environmental Systems Research Institute (ESRI), *ARC/INFO User's Guide: Cell-based Modeling with GRID*, Redlands, Calif., 1991.

EROS Data Center (EDC), *Global 30 Arc Second Elevation Data Set Documentation*, U. S. Geol. Surv. EROS Data Cent., Sioux Falls, S. D., 1996.

Ferrigno, J.G., J.L. Mullins, J. Stapleton, P. S. Chavez Jr., M. G. Velasco, R. S. Williams Jr., G. F. Delinski Jr., and D. Lear, Satellite image map of Antarctica, OPP-9114787, U. S. Geol. Surv., Reston, Va., 1996.

Frederiksen, P., Terrain analysis and accuracy prediction by means of the Fourier transformation, *ISPRS J. of Photogramm. Remote Sens., 36*(4), 145-157, 1981.

Gesch, D.B., and K.S. Larson, Techniques for development of global 1-kilometer digital elevation models, paper presented at Pecora Thirteen Human Interactions with the Environment-Perspectives from Space, U. S. Geol. Surv., Sioux Falls, S. D., August 20-22, 1996.

Horn, B.K.P., Hill shading and the reflectance map, *Geo-Processing, 2*, 65-146, 1982.

Hutchinson, M.F., A new procedure for gridding elevation and stream line data with automatic removal of spurious pits, *J. Hydrol., 106*, 211-232, 1989.

Ihde, J., U. Schirmer, and F. Stefani, Ice mass balance investigation of Antarctica by satellite radar altimeter data, paper presented at The European Conference on Satellite Altimetry, European Community, Las Palmas, Spain, November 20-22, 1995.

Jenkins, A., and C.S.M. Doake, Ice-ocean interaction on Ronne Ice Shelf, Antarctica, *J. Geophys. Res., 96*, 791-813, 1991.

Jezek, K.C., RADARSAT Antarctic mapping project, *Tech. Rep. 17*, Byrd Polar Res. Cent., Ohio State Univ., Columbus, 1998.

Kiernan, R., Ice sheet surface velocities along the Lambert Glacier Basin Traverse Route, *Antarctic CRC Res. Rep.10*, Australian Antarctic Division, Tasmania, in press, 1998.

Lazarev, G.E., Trigonometric leveling on the Komsomolskya-Sovetskaya-Vostok-Komsomolskaya profile (English translation), *Geophys. Bull., 13*, 54-62, 1966.

Liu, H., Generation and refinement of a continental scale digital elevation model by integrating cartographic and remotely sensed data: A GIS-based approach, Ph.D. thesis, Ohio State Univ., Columbus, 1999.

Liu, H., and K.C. Jezek, Investigating DEM error pattern by directional variograms and Fourier Analysis, *Geogr. Anal., 31*(3), 249-256,1999.

Marsiat, I., and J.L. Bamber, The climate of Antarctica in the UGAMP CGM: Sensitivity to topography, *Ann. Glaciol., 25*, 79-84,1997.

Martin, T.V., J.H. Zwally, A.C. Brenner, and R.A. Bindschadler, Analysis and retracking of continental ice sheet radar altimeter waveforms, *J. Geophys. Res., 88*, 1608-1616, 1983.

McDonald, R.A., Opening the cold war sky to the public: Declassifying satellite reconnaissance imagery, *Photogramm. Eng. Remote Sens., 61*(4), 380-390, 1995.

Oswald, H., and H. Raetsch, A system for generation and display of digital elevation models. *Geo-Processing, 2*, 197-218, 1984.

Partington, K.C., W. Cudlip, N.F. McIntyre, and S. King-Hele, Mapping of Amery Ice Shelf, Antarctica, surface features by satellite altimetry, *Ann. Glaciol., 9*, 183-188, 1987.

Phillips, H.A., I. Allison, M. Craven, K. Krebs, and P. Morgan, Ice velocity, mass flux and grounding line location on the Lambert Glacier-Amery Ice Shelf System, Antarctica, *Eos Trans. AGU 77*(22), West. Pac. Geophys. Meet. Suppl., W13, 1996.

Rapp, R.H., Geoid determination, in Report of a Workshop: Utilization of the Global Positioning System (GPS) in Addressing Scientific Problems in Antarctica, *Tech. Rep. 91-02*, edited by D.H. Elliot, W. Strange, and I .M. Willians, pp. 13, Byrd Polar Res. Cent., Ohio State Univ., Columbus, 1991.

Rapp, R.H., Y.M. Wang, and N.K. Pavlis, The Ohio State 1991 Geopotential and Sea Surface Topography Harmonic Coefficient Models, *Rep. 410*, Dept. of Geodet. Sci. and Surv., Ohio State Univ., Columbus, 1991.

Retzlaff, R., N. Lord, and C.R. Bentley, Airborne-radar studies: Ice Streams A, B, and C, west Antarctica, *J. Glaciol., 39*, 495-506, 1993.

Ridley, J.K., W. Cudlip, N.F. McIntyre, and C.G. Rapley, The topography and surface characteristics of the Larsen Ice Shelf, Antarctica, using satellite altimetry, *J. Glaciol., 35*, 299-310, 1989.

Ridley, J.K., S. Laxon, C.G. Rapley, and D. Mantripp, Antarctic ice sheet topography mapped with the ERS-1 radar altimeter, *Int. J. Remote Sens., 14*, 1649-1650, 1993.

Robinson, G.J., The accuracy of digital elevation models derived from digitized contour data, *Photogramm. Rec., 14*(83), 805-814, 1994.

Schutz, B.E., Spaceborne laser altimetry: 2001 and beyond, in Book of Extended Abstracts, edited by H.P. Plag, WEGENER-98, Norw. Mapp. Auth., Honefoss, Norway, 1998.

Shcheglov, S.N., Determination of elevations by the method of geodetic leveling along the Mirnyy-Komsomolskaya traverse (English translation), in *Soviet Antarctic Expedition, Information Bulletin*, vol. 3, pp. 306-310, Elsevier, New York, 1965.

Sievers, J., C.S.M. Doake, J. Ihde, D.R. Mantripp, V.S. Pozdeev, B. Ritter, H.W. Schenke, F. Tyssen, and D.G. Vaughan, Validating and improving elevation data of a satellite image map of Filchner-Ronne Ice Shelf, Antarctica, with results from ERS-1, *Ann. Glaciol., 20*, 347-351, 1994.

Verdin, K.L., and S.K. Greenlee, Development of continental scale digital elevation models and extraction of hydrographic features, paper presented at Third International Conference/workshop on Integrating GIS and Environmental Modeling, U.S. National Cent. for Geogr. Inform. and Anal., Santa Fe, New Mexico, January 21-26, 1996.

Weaver, H.J., *Applications of Discrete and Continuous Fourier Analysis*, John Wiley, New York, 1983.

Yoeli, P., Cartographic contouring with computer and plotte, *Am. Cartogr., 11*, 139-155, 1984.

Zwally, H. J., R.A. Binschadler, A.C Brenner, T.V. Martin, and R.H. Thomas, Surface elevation contours of Greenland and Antarctic Ice Sheets, *J. Geophys. Res., 88*, 1589-1598, 1983.

Zwally, H. J., J. A. Major, A. C. Brenner, T. V. Martin, and R. A. Bindschadler, Ice measurements by GEOSAT radar altimetry, in *The Navy Geosat Mission, Johns Hopkins APL Tech. Dig., 8*(2), 251-254, 1987.

Zwally, H. J., A. C. Brenner, J. DiMarzio, and M. Giovinetto, Ice sheet topography, slopes, and flow directions from ERS altimetery (abstract), *The 3rd ERS Symposium*, Euro. Space Agency, Florence, Italy, March 18-27, 1997.

K. C. Jezek, B. Li, and H. Liu, The Byrd Polar Research Center, Ohio State University, Columbus, OH 43210. (jezek@iceberg.mps.ohio-state.edu; biyanli@iceberg.mps.ohio-state.edu; liu@iceberg.mps.ohio-state.edu)

(Received January 13, 1999; revised June 21, 1999;
accepted June 29, 1999.)